

# Behavior of continuous casting fluxes during heating and cooling

E. BRANDALEZE\*, E. BENAVIDEZ†, L. CASTELLA,\* and J. MADIAS\*

\*Instituto Argentino de Siderurgia, Buenos Aires, Argentina

†Universidad Tecnológica Nacional, Buenos Aires, Argentina

Knowledge of the physical and chemical properties as well as the behaviour of the mould fluxes during melting, important in order to improve continuous casting operations. Lubrication and control of heat transfer in the mould are the more relevant functions of these materials. Values of physical properties like viscosity and surface tension at melting range temperatures are required, as much as the thermal behaviour under process conditions.

The heat extraction from the liquid steel has an important effect in the final quality of products. Mould fluxes are constituted by different oxides, and may form glasses and crystal phases during cooling. The solidification rate and the chemical composition determine the proportion, type and crystalline morphology, which are responsible of the thermal transfer processes.

In this paper, viscosity values are reported in the melting range temperatures calculated by means of the Riboud model and compared with fluidity results obtained by the inclined plane technique. Also the linear expansion of the mould fluxes at high temperatures was determined by dilatometry. The crystallization in two different fluxes was determined by DTA tests and correlated with the basicity index. Crystal phases were evaluated by scanning electronic microscopy on quenched samples at 1300°C. This information is relevant to increase the knowledge on the peritectic steel grades casting process in order to improve its quality.

Keywords: mould fluxes, heat transfer, crystal phases, peritectic steels, thermal properties.

## Introduction

In the continuous casting process the molten steel is delivered through a submerged entry nozzle into a mould. The steel against the mould freezes; the shell is formed. Mould fluxes are placed on the top of the liquid steel to bring about lubrication and to control the heat transfer process.

Sticking and cracking phenomena are particular problems determined by the interruption of the molten slag flow. As a consequence, thermal stresses in the shell appear and are the results of different thermal contraction coefficients between ferrite and austenite phases. A high value of heat flow is related to surface defects, especially for peritectic steel grades. Therefore knowledge of the amount of crystal phases in the slag film is a fundamental step in developing or mould flux selection in connection with these steel grades and operating parameters.

Recent literature has focused attention on the properties of solidifying liquid slag. Nevertheless, traditional data on melting behaviour of mould fluxes such as softening, melting and flow point are relevant and constitute a complementary knowledge to understand the key parameters to control strand lubrication and heat flow between the strand and mould wall.

This paper focuses on the relation among basicity, the amount of crystal phases, thermal properties and heat transfer referred to slab casting in peritectic grades.

## Experimental

Two different mould fluxes, A and B, selected for this study, are used in the peritectic grades casting process. The chemical compositions of both fluxes are presented in Table I.

Table I  
Chemical composition of mould fluxes type A and B.

Composition (%)	Mould Fluxes	
	A	B
SiO <sub>2</sub>	30.50	32.60
CaO	33.50	41.10
Al <sub>2</sub> O <sub>3</sub>	6.30	3.70
MgO	1.04	2.70
MnO	0.03	–
TiO <sub>2</sub>	0.01	0.1
K <sub>2</sub> O	0.12	0.06
Fe <sub>2</sub> O <sub>3</sub>	1.14	0.54
Na <sub>2</sub> O	6.80	5.50
F	7.20	7.85
Free C	7.91	3.78

**Table II**  
Values of basicity, viscosity and system thermal conductivity

Properties	Mould Fluxes		
	A	B	
Binary basicity index	1.09	1.26	
Basicity $B_i$ (Branion) <sup>2</sup>	1.77	1.68	
Viscosity at 1300°C (Riboud) <sup>3</sup> (dPa•s)	1.15	0.62	
Long. inclined plane, 1300°C (mm)	32.2	34.8	
$K_{sys}$ System conductivity <sup>4</sup> ( $Wm^{-1}K^{-1}$ )	1.10	1.16	
Critical temperatures	IT °C	1097	1181
	ST °C	1130	1184
	HT °C	1147	1198
	FT °C	1157	1218

Other relevant data for melting fluxes behaviour are the critical temperatures. The fusibility of both powders was measured by a Leco (AF-500) instrument. Powders were prepared with a few drops of 10% solution of dextrin containing 0.1% salicylic acid as a preservative. These blends were pressed into a cone mould using a spatula. The dried cones were removed from the mould and the critical temperatures, initial temperature ( $T_i$ ), softening point ( $T_s$ ), hemispherical point ( $T_h$ ), and fluid point ( $T_f$ ), were determined.

The fluidity of both mould fluxes was determined by means of the inclined plane technique developed by Mills<sup>1</sup>. Samples of 10 g were melted in a platinum crucible up to 1300°C. After 15 min of maintenance at this temperature they were poured over a plane inclined 10 degrees. The longitude of the mould flux layer formed was measured by a caliber. Averages of several tests were considered in this work to correlate with basicity, and physical and thermal properties. The layers obtained, were cut and prepared for a dilatometry test.

Cross-sections of the solidified layers were prepared for microscopy observation. To enhance the observation of crystal phases, all the samples were attacked with nital. Because of the high proportion of vitreous phases observed in both types of materials, a second attack with FH acid was carried out. The study by an electronic microscope Philips 505, led us to identify crystal phases and determine the chemical composition using EDS.

The dilatometries were carried out by horizontal Theta Dilatronic II equipment. Samples with longitudes between 10 and 20 mm were tested. The heating rate was 10 °C/min. It is important to mention that the test was carried out up to the temperature at which a contraction of the sample was observed.

Simultaneous DTA-TG measurements by a Netzsch STA 409/c analyser were carried out on samples of 200 mg of each mould flux. A normal atmosphere and a temperature range between room temperature and 1255°C were used. The fluxes were tested in a Pt-Rh crucible and alumina was used as a reference material. The heating

rate selected was 10°C/min and the cooling rate of 5°C/min.

## Results

### Properties related to the chemical composition

According to the mould flux compositions some properties were calculated. Table II shows the binary index ( $CaO/SiO_2$ ) and basicity index ( $B_i$ ) calculated by equation [1]<sup>2</sup>

$$B_i = \frac{1.53\%CaO + 1.51\%MgO + 1.94\%Na_2O + 3.55\%Li_2O + 1.53\%CaF_2}{1.48\%SiO_2 + 0.10\%Al_2O_3} \quad [1]$$

Viscosity at 1300°C was obtained by the Riboud model<sup>3</sup> and the system conductivity ( $K_{sys}$ ) of each mould flux was obtained according to Holzhauser *et al*<sup>4</sup>. These values are presented in Table II. Critical temperatures corresponding to A and B fluxes are also shown in Table II.

### Differential Thermal Analysis and Thermogravimetry

DTA-TG heating curves for the mould flux A are presented in Figure 1. As one can see, an exothermic peak appears at 410°C for this material. From this temperature up to 840°C a series of exothermic reactions occur accompanied by a mass loss. In the range between 410 – 840°C the weight loss is 12.3%. At higher temperatures the mass of material remains without changes. Deriving the TG-curve (curve DTG in Figure 1) three peaks can be identified at the following temperatures: 495°C, 557°C and 722°C. Therefore, at these temperatures the highest rates of mass loss are presented. At higher temperatures than 1000°C, the DTA-curve presents two small endothermic peaks.

The DTA cooling curve (Figure 2) shows two exothermic peaks, the first one at 1153°C and the second one at 946°C. Throughout the cooling period of mould flux A, the weight remains constant (not shown in the Figure 2).

The curves of DTA-TG corresponding to the heating of mould powder B are presented in Figure 3. In this case, the exothermic reactions take place from 150°C to 780°C. Four peaks were clearly identified in the DTA curve. These reactions coincide with an increase in the loss mass rate (curve DTG) and they are accompanied by a continuous lost of weight. At higher temperatures a negligible weight loss (approx. 0.5%) took place.

The cooling cycle of sample B, does not present

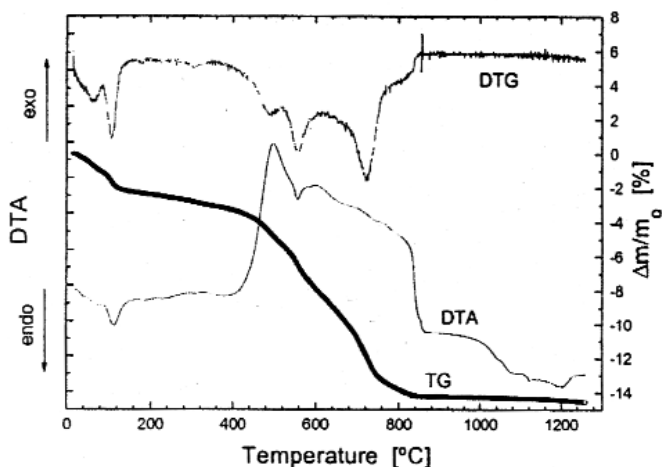


Figure 1. DTA-TG curves for mould flux A

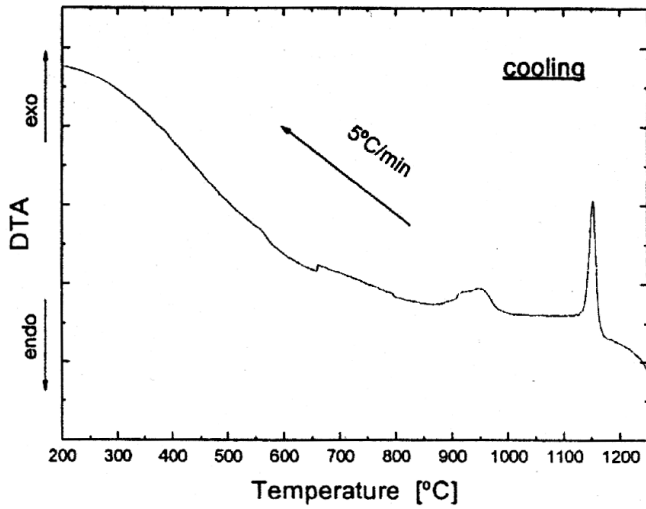


Figure 2. DTA cooling curve for the mould flux A

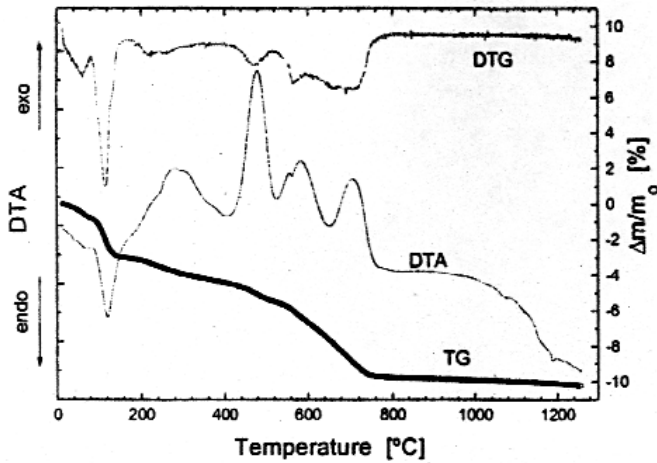


Figure 3. DTA-TG curves for mould flux B

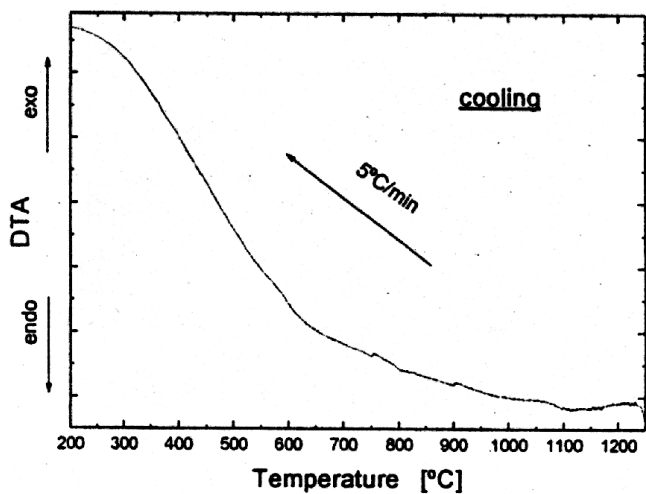


Figure 4. DTA cooling curve for mould flux B

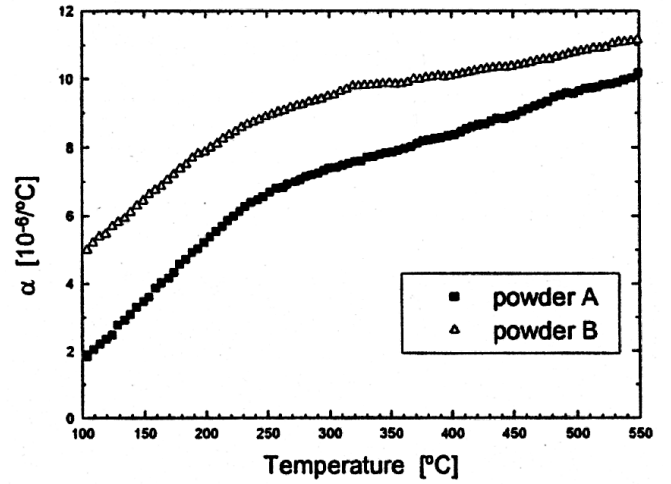


Figure 5. Linear expansion coefficient of sample A and B.

exothermic peaks indicating any crystallization reaction. Similar to sample A, there is no change in the weight during the cooling of sample B (not shown in Figure 4).

#### Dilatometric analysis

Dilatometric runs were carried out on samples A and B, the linear expansion coefficient ( $\alpha$ ) can be calculated. The  $\alpha$  values corresponding to samples A and B are shown in Figure 5. A smaller value of the linear expansion coefficient of sample A is observed throughout the temperature range analysed.

As it is possible to see, both mould fluxes have linear expansion coefficient values that increase continuously during the heating. At first, up to 250°C, the values of  $\alpha$  increase rapidly, and then between 250–550°C they increase more gradually. At temperatures higher than 545°C for

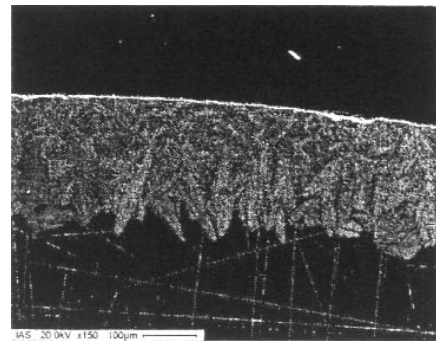


Figure 6. Aspect of general microstructure of flux A [150x]

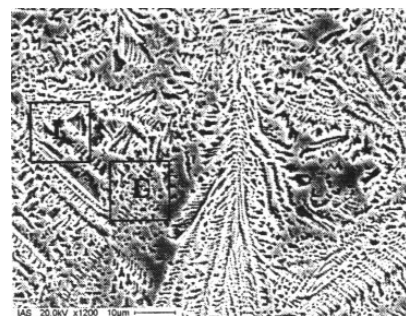


Figure 7. Dendrite detail [1200x]

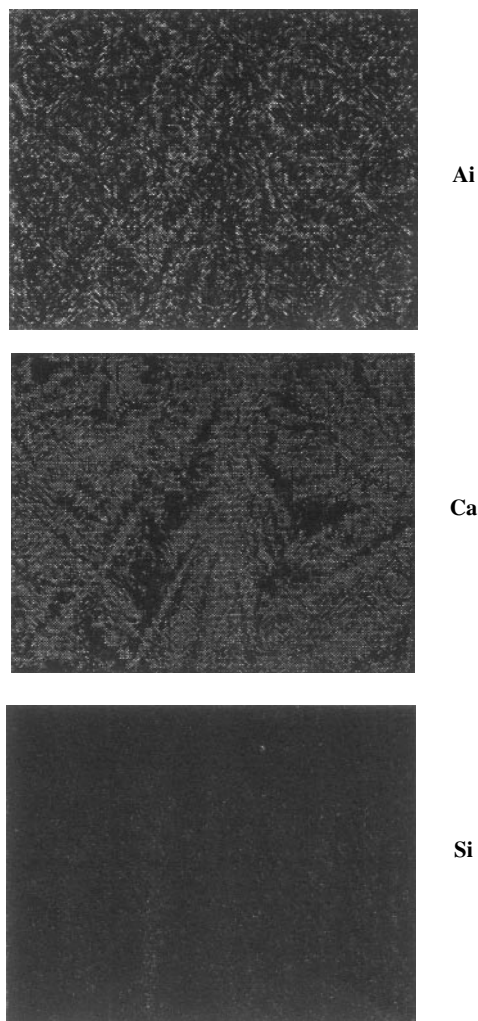


Figure 8. Mapping of elements in the glass layer

sample A (and 575°C for sample B), the dilatometric curve shows an important increase in its expansion rate. This anomalous behaviour is associated with the glass transition temperature ( $T_g$ ) of the vitreous phase present in both samples <sup>5</sup>.

#### Electronic microscopy

SEM studies on mould flux A sample, permit one to determine a large amount of vitreous phase. A thin dendrite crystal layer was formed in a localized area of the sample surface. A general microstructure of the crystalline and glass phases is observed in Figure 6.

In Figure 7, dendrite crystal details are observed. The chemical composition of the dendrite crystal (D) and the interdendritic liquid (I) were determined by EDS; results are shown in Table III.

Maps corresponding to Al, Ca and Si elements are presented in Figure 8.

Material	Na <sub>2</sub> O (%)	MgO (%)	Al <sub>2</sub> O <sub>3</sub> (%)	SiO <sub>2</sub> (%)	CaO (%)	FeO (%)
I	6.0	–	12.9	48.7	31.1	1.3
D	7.2	3.3	14.2	50.0	24.2	–

Table III

Dendrite and interdendritic liquid chemical composition of flux A

In material B, more vitreous phase without a crystalline layer was formed; only isolated crystals next to the surface were observed, as it is shown in Figure 9.

The dendrite morphology is shown in Figure 10. The chemical composition of dendrite and interdendritic zones was analysed by SEM/EDS and they are presented in Table IV.

Maps of Al, Ca and Si of the crystal can be observed in Figure 11.

### Discussion

The heat flow balance and the lubrication effect in the continuous casting process are the major problems for medium C, low C, and peritectic steel grades. The precipitation of crystalline phases whose proportion increases with basicity<sup>6</sup> causes thermal heterogeneity and poor lubrication. According to the values of binary basicity, a large amount of vitreous phase should be developed in both powders. However, values of the  $B_i$  basicity obtained contemplates the whole chemical composition and permits one to think that the crystallizing tendency will be higher in mould flux A than in B.

According to SEM observations, flux B presents a very low proportion of crystalline phase, which is confirmed, for the crystallization peaks obtained during its cooling cycle by DTA. This material presents small, isolated and dispersed crystals on the surface. The higher proportion of vitreous phase promotes the radiation heat transfer contribution and the conduction by phonon mechanism can be neglected.

Although powder A presented crystallization peaks during its cooling cycle, the microstructure observations also showed a scarce presence of crystals. However, in this sample the crystals were detected in a greater proportion than in B. At high temperatures, the heat transfer by the radiation mechanism prevails over that by conduction.

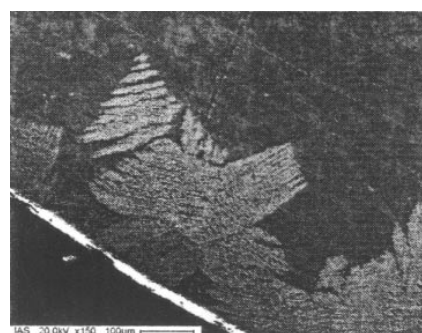


Fig 9. Aspect of the flux general microstructure. [150x]

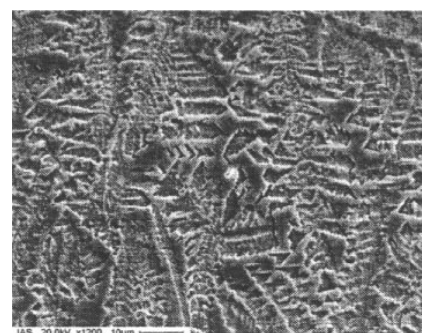


Fig 10. Dendrite detail. [1200x]

**Table IV**  
**Dendrite and interdendritic liquid chemical composition of flux B**

Material	Na <sub>2</sub> O (%)	MgO (%)	Al <sub>2</sub> O <sub>3</sub> (%)	SiO <sub>2</sub> (%)	CaO (%)	FeO (%)
B						
I	–	–	5.5	47.7	46.2	0.64
D	5.1	6.3	10.1	53.8	25.5	–

According to these results, the conduction component of heat transfer would not be important in both samples. This fact permits one to think that, in the initial instants of the process, the slab will freeze rapidly using both material A and B.

It is known that peritectic steels are susceptible to cracking. In general these cracks are generated because of thermal stress generated in the shell, resulting from differences in thermal contraction between ferrite and austenite phases<sup>7</sup>. Differential contractions promote the early separation between metal and mould, that it can be reverted through a thicker mould powder layer but with a low viscosity<sup>5</sup>.

Both powders have low viscosity at 1300°C and the smaller value is for powder B. The viscosity, calculated in theoretical form, can be experimentally confirmed by the inclined plane tests. A longer layer confirmed a higher fluidity for the powder B. Also, the lower linear expansion coefficient of the material A ( $\alpha$ ) indicates that this material has a structure that does not allow an easy displacement of the SiO<sub>4</sub><sup>2-</sup> tetrahedra. At higher temperature, when the powder is molten, this structure means a higher viscosity. This finding is consistent with the binary index but not with the Bi index.

The penetration of the liquid slag and the thickness of the formed layer between the shell and the mould ( $d_{cf}$ ) are factors that influence the lubrication process during the steel casting. These conditions are largely dependent on the viscosity of the mould fluxes at high temperatures. It is known that a higher viscosity generates a thicker layer of fluxes when they are flowing between the shell and the mould. Due to the smaller viscosity of powder B than of powder A, it should be expected that the layer formed by powder B is thinner. Also, the thermal conductivity of the system calculated for powder B,  $k_{sys}(B)$ , is higher than  $k_{sys}(A)$ . Therefore, using the expression for heat flow  $q = (k_{sys}/d_{cf}) \cdot \Delta T_m$ , it is expected that the heat extraction would be faster with material B.

According to the relationship<sup>7</sup>:  $\eta \cdot V_c \approx 2$  it is advisable that mould flux B should be cast at a faster rate than A. The higher casting rate associated with mould flux B is also possible because this powder B allows a higher speed of heat extraction.

## Conclusions

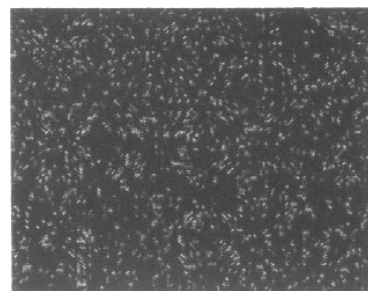
Dilatometric assays and an inclined plane test demonstrated their usefulness to confirm calculated fluidity and viscosity.

A higher crystallization grade was determined in powder A from DTA runs and microstructural observations.

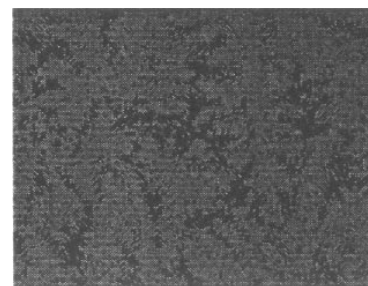
From the results obtained in this work it can be inferred that both powders A and B can be used in continuous casting of peritectic steel slabs, taking into account that a higher casting speed for the mould powder B should be considered.

## References

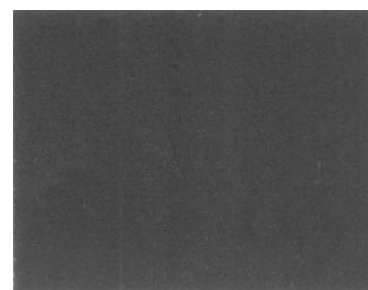
1. MILLS, K.C., HALALI M., LÖRZ H.P., *et al.*, A



Ai



Ca



Si

**Figure 11. Mapping of elements in the crystals of flux B.**

Simple test for the measurement of slag viscosities. *5th Conference on Molten Slags, Fluxes and Salts*, 1997, pp. 535–542.

- BRANION R.V., Mold Fluxes for Continuous Casting, *Iron and Steelmaking*, September, 1986, pp. 41–50.
- RIBOUD P. V., Continuous casting slags. *Seminaire: Formation de la première peau en coulée continue*, Institut de Recherches de la Sidérurgie Française IRSID, 1985, pp. 1–30.
- HOLZHAUSER J.F., SPITZER K.H. and SCHWERDTFEGER K. Study of heat transfer through layers of casting flux: experiments with a laboratory set-up simulating the conditions in continuous casting. *Steel Research*, vol. 70, no. 7, 1999, pp. 252–258.
- J. HLAVAC, *The technology of glass and ceramics: An introduction*, Elsevier Scientific Publishing Company, New York, 1983.
- CARLI R. and GHILARDI V., Managing Technological Properties of Mold Fluxes, *Iron and Steelmaking*, 1998, pp. 43–46.
- CHAVEZ J.F., RODRIGUEZ A., MORALES R. and TAPIA V., Laboratory and plant studies on thermal properties of mold powders. *Steelmaking Conference*, 1995, pp. 679–686.
- MILLS K.C. and FOX A.B. Mould Fluxes, *Mills Symposium*, V 1, London, 2002.

